Experimental Analysis of Synchrophasing Impact on Noise of Distributed Propeller Systems in Tractor Configuration

Experimental Analysis of Synchrophasing Impact on Noise of Distributed Propeller Systems in Tractor Configuration

Fernanda do N. Monteiro*, Ramon R. Duivenvoorden †, Daniele Ragni ‡ and Tomas Sinnige §
Delft University of Technology, Delft 2629HS, The Netherlands

Francesco Avallone ¶
Polytechnic of Turin, Turin, 10129, Italy

This study investigates the acoustic characteristics of a distributed propeller-wing system in a tractor configuration, focusing on the potential for noise reduction using the synchrophasing technique. The experimental setup features three propellers with nacelles mounted side-by-side on the leading edge of a wing, resulting in aerodynamic interference between adjacent propellers due to a tip clearance of 5% of the radius. The study investigates the acoustic impact of varying relative blade-phase angles (synchrophasing) and further explores the implications of changing the angle of attack. The findings show that synchrophasing influences noise emissions at the locations investigated, potentially amplifying or reducing noise relative to a random configuration. Moreover, these effects persist when investigating higher angles of attack.

Nomenclature

BPF	=	blade-passing frequency, Hz
d	=	separation distance between propellers, m
D	=	propeller diameter, m
f	=	frequency, Hz
J	=	advance ratio
n	=	rotational speed, Hz
PDS	=	power spectral density, dB/Hz
p_{ref}	=	reference sound pressure, Pa
r	=	blade radial coordinate, m
R	=	propeller radius, m
RPS	=	revolutions per second, Hz
SPL	=	sound pressure level, dB
T_c	=	$= T/(q_\infty D^2)$, propeller thrust coefficient based on freestream dynamic pressure
U_∞	=	freestream velocity magnitude, m/s
X, Y, Z	=	Cartesian coordinates, m
α_w	=	wing angle of attack, $^\circ$
β	=	blade pitch angle, $^\circ$
$\Delta\phi$	=	relative blade-phase angle, $^\circ$

I. Introduction

Over recent years, the environmental impact of the air transport industry has drawn significant public concern. In response, international organizations have set specific targets to reduce pollution and noise caused by aviation. One such initiative is the Flightpath 2050 strategy, which aims to significantly reduce CO_2 and NO_x emissions and perceived

*PhD candidate, Wind Energy Section, Fac. of Aerospace Eng., F.doNascimentoMonteiro@tudelft.nl, AIAA Member.
†PhD candidate, Flight Performance and Propulsion Section, Fac. of Aerospace Eng., R.R.Duivenvoorden@tudelft.nl, AIAA Member.
‡Associate Professor, Wind Energy Section, Fac. of Aerospace Eng., D.Ragni@tudelft.nl, AIAA Member.
§Assistant Professor, Flight Performance and Propulsion Section, Fac. of Aerospace Eng., T.Sinnige@tudelft.nl, AIAA Member
¶Full Professor, Department of Mechanical and Aerospace Engineering, Polytechnic of Turin, Francesco.Avallone@polito.it, AIAA Member.

noise levels from aircraft by the year 2050 [1]. To support this cause, the International Air Transport Association (IATA) has developed a series of roadmaps to achieve net-zero carbon emissions by 2050. These Net Zero Roadmaps focus on aircraft technology, energy infrastructure, operations, finance, and policy. One of the critical milestones on the Technology Roadmap is the introduction of Distributed Propulsion (DP) demonstrators for commuter aircraft and Urban Air Mobility (UAM) between 2023 and 2030 [2].

One promising configuration is adopting Distributed Electric Propulsion (DEP) systems. These systems strategically place propulsors across the airframe, enhancing several vehicle aspects, including aerodynamics, structural design, control, and possibly acoustic emissions [3–5]. However, it is crucial to understand what noise sources dominate under specific operating conditions and their directivity for particular vehicle configurations. For instance, coherent sources like propellers operating at the same RPM can generate complex directivity patterns, which become particularly challenging to predict when transitioning from ideal to realistic flight conditions, such as error in the rotational speed control [6]. Installation or interaction effects can also significantly change harmonic content under certain circumstances [7, 8].

Distributed propeller systems in a tractor configuration present a promising area of research due to their potential benefits. Strategically placing propellers upstream of the wing can increase the wing's lift by blowing air over its surface. This increases the inflow velocity over the wing, thereby generating more lift [3]. Moreover, the placement of propellers can also improve the overall efficiency by reducing drag, as the propellers can re-energize the boundary layer on the wing, delaying or preventing flow separation [3]. However, multiple propellers can generate significant noise levels.

As a potential solution, synchrophasing could help reduce noise in distributed propeller systems. Phase control, or synchrophasing, involves controlling the blade's relative phase angle between propellers. This approach uses the destructive interference of the coherent acoustic source field. Though this is not a new idea—it is used in traditional aircraft to lower cabin noise[9–11]—synchrophasing has gained renewed interest for its potential to reduce noise in communities near airports [6, 12–14]. However, errors in motor controllers can degrade this ideal benefit [6]. Also, unsteady blade loading, which can result from installation [15–18] or interaction effects [19–21], could significantly alter the noise at blade passing frequency and its harmonics.

Though previous studies have investigated the noise produced by an array of propellers and the impact of synchrophasing [6, 20, 22], it needs to be still clarified if the noise reductions from synchrophasing persist when a wing is positioned downstream of the propeller array, thereby impacting the system's acoustics and In order to address this gap, we performed a wind tunnel experiment using a set of three identical propellers in a tractor configuration. We aimed to determine whether synchrophasing helps in noise reduction, and to identify the sensitivity of this technique.

The remainder of this paper unfolds as follows. Section II provides a comprehensive look at the experimental methodology, covering aspects such as the test facility, the acoustic test section, the model, the test conditions, and the methodology adopted in carrying out and post-processing the acoustic measurements. Section III initially presents the results from the baseline configuration, followed by the findings after an increase in the wing's angle of attack. Lastly, section IV discusses the key results, remarks concerning the data presented, and a glance into potential routes for future research.

II. Experimental Methodology

A. Wind Tunnel and Acoustic Test Section

The experiments were performed at the Low-Speed, Low-Turbulence Tunnel (LTT) at Delft University of Technology (TU Delft). The LTT is a closed-circuit wind tunnel that can reach a maximum freestream velocity of 120 m/s. At the freestream velocity used in these experiments, the turbulence levels are below 0.04% [23]. Its test section has an octagonal cross-section that measures 1.8 m wide, 1.25 m high, and 2.60 m long.

Originally designed for aerodynamic studies, this wind tunnel is not ideally suited for acoustic measurements. Its closed-loop structure causes acoustic reflections within the circuit, resulting in a long reverberation time. To mitigate this issue, an acoustically treated test section was employed (Fig. 1). This test section was designed to minimize acoustic reflections, specifically those that follow a direct path from the noise sources to the microphone array [24, 25]. The enhancements include a 3 cm layer of melamine foam on the ceiling and floor. The sidewalls were fitted with a 5 cm thick layer of wedged melamine, covered by a Kevlar sheet, except for the wall where the microphones were mounted, which has a window solely covered by a tensioned Kevlar sheet. The microphone array was positioned behind this Kevlar window and lined with 5 cm of melamine for improved sound absorption. Ramps were placed upstream and downstream of the melamine panels on the floor and the ceiling to prevent strong aerodynamic loads from impinging the

lining and potentially increasing background noise.

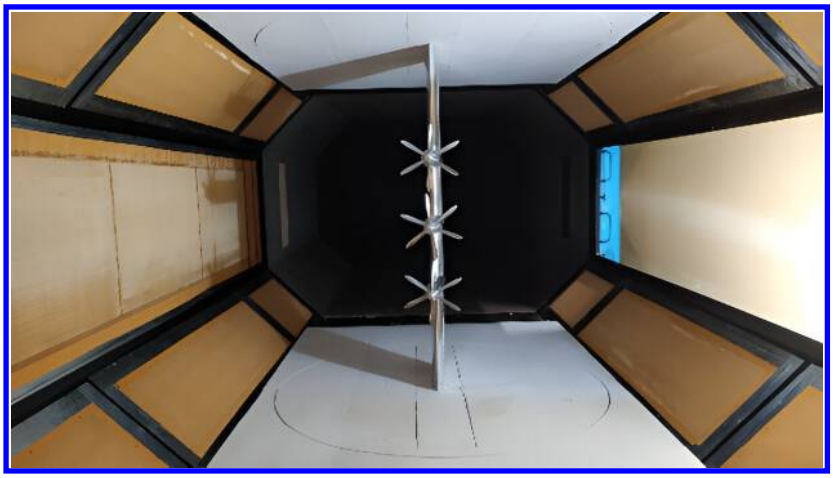

Fig. 1 Acoustic test section of the LTT.

B. Model Description

The model features three propellers, installed side by side on the leading edge of an unswept, untapered wing (see Fig. 2). These propellers, referred to as TUD-XPROP-S [26], are made of steel, consist of six blades, and have a diameter of $D = 203.2$ mm. The blade pitch was set to 30° at 70% of its radius. Additional propeller information can be found in the work of van Arnhem et al. [27]. For information on the propellers' aerodynamic performance in a distributed configuration, see the experimental study by de Vries et al. [20].

The wing has 0.3 m of chord and 1.248 m of span. It features an NLF-Mod22(B) [28] airfoil, which has a maximum thickness-to-chord ratio of 0.17 at 35% chord and a Fowler flap, which remained nested throughout the experiment. The gap between the main wing and the flap was covered with metallic tape to prevent undesirable noise sources.

Each propeller was powered by a Lehner LMT 2260/40 motor, housed in an aluminum nacelle set at a 5-degree downward angle relative to the wing's chord, with its own trapezoidal electronic speed controller (ESC) controlled by pulse-width modulation (PWM) and a programmable 5 kW DC power supply.

The propellers were positioned at approximately $0.85D$ from the wing's leading edge. The middle propeller and nacelle were mounted on the wing centerline, while both side propellers were installed with a minimum tip clearance of about 5% of the propeller radius. The wing was mounted vertically in the center of the test section and clamped to the wind tunnel bottom and floor. An overview of the model characteristics is presented in Table 1.

Table 1 Model characteristics

Propellers		Wing	
Diameter, D [m]	0.2032	Chord, [m]	0.3
Blade pitch, $\beta_{0.7R}$ [deg]	30	Span, [m]	1.248
Number of blades [-]	6	Taper ratio, [-]	0
Number of propellers [-]	3	Sweep angle, [deg]	0
		Airfoil	NLF-Mod22(B)

C. Test Conditions

The freestream velocity was maintained at 30 ± 0.01 m/s throughout the acoustic measurements. The measured freestream's static pressure, density, and temperature were 1011.16 hPa, 1.198 kg/m^3, and 293.98 K, respectively.

The propellers were co-rotating (see Fig. 2) and their blade pitch was set at $0.7R$ to $30° \pm 0.05°$. In the case of TUD-XPROP-S, this pitch setting provides maximum efficiency at high thrust settings, which represents take-off

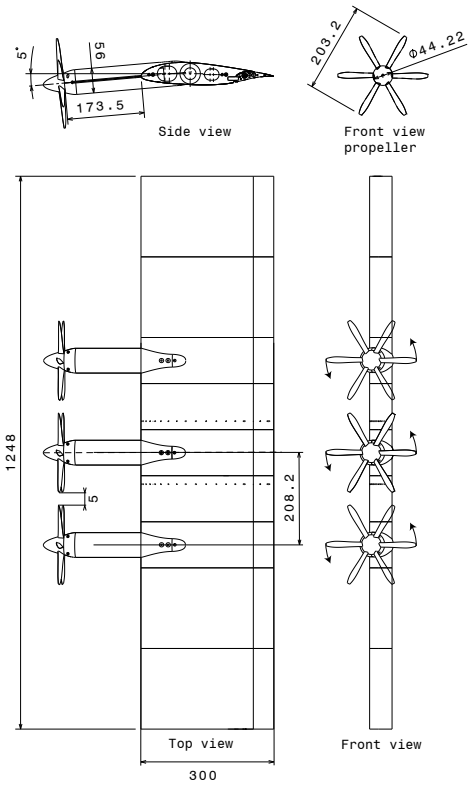

Fig. 2 Technical drawing (dimensions in mm)

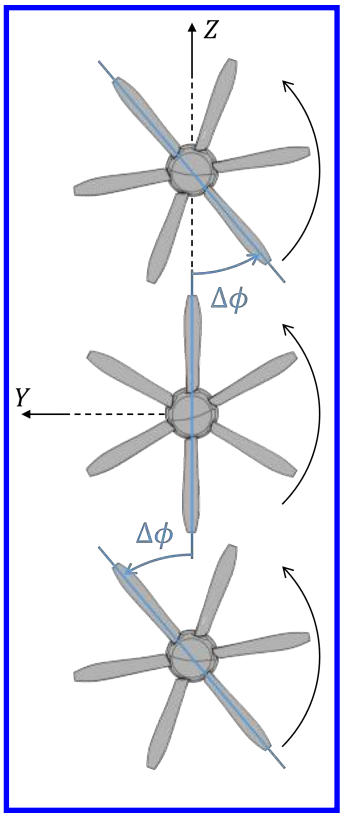

Fig. 3 Definition of $\Delta\phi$ (front view).

conditions, as in the study of de Vries et al. [20]. However, this angle was chosen over larger pitch angles because the higher thrust coefficients and blade tip Mach numbers make the aerodynamic and acoustic interaction effects more prominent in the experiment.

Due to the constraints of the electric motor, the propellers were limited to operating at an advance ratio of $J = 0.8$ (184.5 Hz). This value corresponds to isolated-propeller thrust coefficients of $T_c = 1.05$. At this advance ratio and freestream condition, the helical tip Mach number is 0.36, and the Reynolds number at the tip is approximately 6.0×10^4.

Control over the rotational speed and the relative blade phase angle among propellers was achieved via software developed in-house. The standard deviation of the rotational speed was 0.01 Hz during measurements. The relative blade-phase angles $\Delta\phi$ (see Fig. 3) were varied from 0° to 50° in 10° increments. The standard deviation of the relative blade-phase angle during the phase-controlled measurements was below 0.16°, demonstrating that the controller was accurate enough to study the impact of relative blade-phase angles on noise production without any significant loss in coherence of the noise sources [6]. Measurements were also taken with a random relative blade phase angles between all propellers. This was achieved by slightly increasing the rotational speed of the side propellers by 0.03 Hz relative to the middle propeller, which had an insignificant effect on the propeller's performance. Hence, minor variations in the propeller's rotational speed are not likely to noticeably impact the blade loading. As a result, this should not lead to significant changes in the noise sources or the overall noise output of the propeller system.

Lastly, the wing's angle of attack was adjusted from 2° to 8° degrees with a precision of ±0.01°. An overview of the test conditions is presented in Table 2.

D. Acoustic Data

The experimental campaign utilized a microphone array comprised of 64 *G.R.A.S. 40PH* analog free-field microphones, arranged in a specific configuration that extended 1.5 m in the streamwise direction and 0.4 m along the spanwise direction (see Fig. 4). The microphones were recessed 15 cm from the Kevlar side wall and facing the pressure side of the wing. The array's center microphone is aligned with the wing's rotational axis at one-quarter of the wing chord. This arrangement placed most upstream and downstream microphones at an angle of ±40° from the turning axis,

Table 2 Overview of test conditions

Parameter	Evaluated values	Baseline value
Freestream velocity, U_∞ [m/s]	30.0	30.0
Wing angle of attack, α_w	2°, 5°, 8°	2°
Blade pitch at $r/R = 0.7$, $\beta_{0.7R}$[°]	30	30
Advance ratio, J [-]	0.80	0.80
Relative blade-phase angle, $\Delta\phi$ [°]	random, 0, 10, 20, 30, 40 and 50	random
Rotation direction	co-rotating	co-rotating
Minimum tip clearance d [mm]	4.8	4.8

and along the span, the maximum angle covered was ±22° from the central propeller. Each measurement lasted 30 seconds and had a sampling frequency of 51.2 kHz. The system also synchronously recorded the pulses from each motor's encoder with the signals of the 64 microphones. This acoustic data acquisition was controlled with a *National Instruments* (NI) four *PXIe-4499* sound and vibration modules with 24-bit resolution and a maximum sampling rate of 204.8 kHz. An *NI RMC-8354* computer controlled these modules via an *PXIe-8370* board.

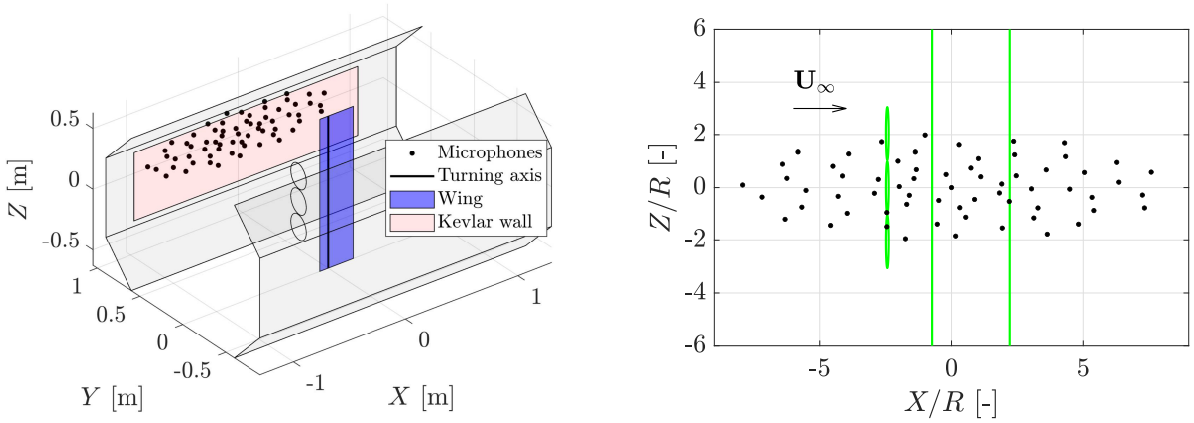

(a) Pressure side measurements. **(b) Side view.**

Fig. 4 Microphone array positioning on the pressure side.

The acoustic data was processed through a spectral analysis using Welch's method, which computes the Power Spectral Density (PSD) with an 8192 block length, 0.5 overlap, and filtered by a Hanning window, resulting in frequency spectra with a frequency resolution of $\Delta f = 6.25$ Hz. Following this, the acoustic signals from the microphones were converted into the Sound Pressure Level (SPL, in dB):

$$\mathrm{SPL} = 10 \log_{10} \frac{\mathrm{PSD}(f)\,\Delta f}{p_{\mathrm{ref}}^2} \tag{1}$$

where $p_{\mathrm{ref}} = 20\,\mu$Pa. To obtain the Overall Sound Pressure Level (OSPL) the SPL results were integrated in the frequency corresponding to $0.9 \leq \mathrm{BPF} \leq 10$, where BPF is the blade-passing frequency.

III. Results

A. Baseline Configuration Analysis

In a tractor configuration, the upwash effect of the wing influences the propeller's performance. This effect is attributed to the changes in the flow direction upstream from the wing, which subsequently alters the local angle of

attack that the propeller blades experience during a revolution [29]. However, this paper aims not only to understand the wing impact on the acoustic emissions of a distributed propeller system but also to analyze the significance of rotor-rotor interferences. In an effort to separate these effects, the wing angle of attack was chosen so that the upwash effect in the upstream propellers aligns the local flow direction with the propeller's incidence angle. Consequently, although the propellers still experience the blockage effect of the downstream wing, the fluctuations induced by the wing in the blade's local angle of attack during a single rotation are minimized. This setting allows for a more efficient study of the impact of rotor-rotor interference. In the case of this experimental model and at a freestream speed of 30 m/s, this alignment takes place when the wing's angle of attack is 2°. Therefore, this angle of attack is chosen as the baseline.

Microphones A, C, and D were selected for preliminary analysis to evaluate the effects of synchrophasing in a distributed-propeller system setup (see Fig. 5). These microphones are positioned near the $Z/R = 0$ axis and side distance $Y/R = 10.3$. Using as reference $X/R = 0$, microphone A is located upstream with a propagation angle of 52°, whereas a propagation angle of 0° would be directly upstream of the middle propeller axis. Microphone C corresponds to a propagation angle of 90° and microphone D is placed downstream with a propagation angle of 125°. The vertical distances from the $Z/R = 0$ axis for microphones A, C and D are $Z/R = 0.098$, 0 and -0.3, respectively.

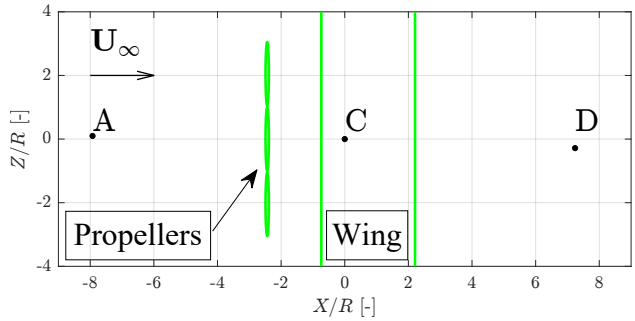

Fig. 5 Positions of microphones A, C and D.

Initially, an analysis was performed on the acoustic signals from microphone C (Fig. 6). This analysis focused on the OSPL and SPL at the first harmonic across different relative blade-phase angles, and also a random case. The relative blade-phase angle impacted both the OSPL and the first BPF, where the highest values were measured at $\Delta\phi = 0°$. These values then decreased to their lowest at $\Delta\phi = 30°$, before increasing again for higher relative blade-phase angles. Compared to the random setting, $\Delta\phi = 0°$ resulted in a 3 dB increase in OSPL and a 4 dB increase at the first BPF. Conversely, $\Delta\phi = 30°$ caused a 3 dB decrease in OSPL and an 8 dB decrease at the first harmonic. Therefore, compared to the random case, the relative blade phase at this location can increase or decrease noise depending on its value. The differences between measurements at $\Delta\phi = 0°$ and $\Delta\phi = 30°$ could be as high as 6 dB in OSPL and 13 dB at the first BPF.

Changes in noise levels are expected not only from the acoustic interference of multiple noise sources but also due to the impact that periodic loading has on the noise sources strength. At $\Delta\phi = 0°$, aerodynamic interference between adjacent propellers should reach their maximum, leading to higher noise levels. However, these interference are minimized at $\Delta\phi = 30°$, resulting in quieter levels. Figure 7 shows the spectra recorded at microphone C for different relative blade-phase angles, including a random case. Significant differences were observed with changes in the relative blade-phase angle, where for the first three harmonics, the highest values are obtained at $\Delta\phi = 0°$, and the lowest are obtained at $\Delta\phi = 30°$, and in between them, there are the harmonics of the random case. Multiple peaks were observed between the BPF multiples and at its subharmonics, though they were significantly less prominent when compared to the harmonics acoustic levels. These peaks are multiples of the shaft frequency and could be attributed to minor blade imbalances and vibrations of the setup [20, 30].

Figure 8 further explores the impact of variations in the relative blade-phase angle on noise emissions in the streamwise direction. At first glance, a general increase of noise levels from the upstream microphone to the downstream microphone is evident, with an average OSPLs of 73 dB upstream increasing to 76 dB downstream. The same trend observed in microphone C is mirrored here, where the sound level is increased at $\Delta\phi = 0°$, while there is a noise reduction at $\Delta\phi = 30°$ when compared to the random case. Nevertheless, the impact on noise at the downstream microphone is more pronounced. For the OPSL values upstream, there is a marginal difference of 1.5 dB between $\Delta\phi = 0°$ and $\Delta\phi = 30°$, but downstream, this difference escalates to 6 dB. For the first harmonic, the difference upstream between $\Delta\phi = 0°$ and $\Delta\phi = 30°$ is 5.5 dB, whereas downstream, this difference increases to 12 dB. When compared to

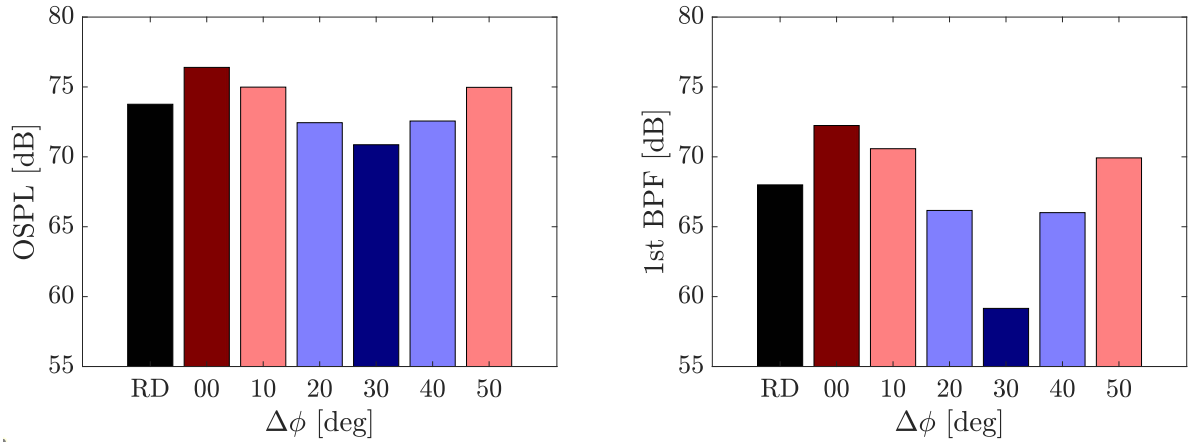

(a) Changes in OSPL. **(b) Change in the first BPF.**

Fig. 6 Changes in OSPL and first BPF at various $\Delta\phi$ at microphone C (BPF = 1107 Hz, $J = 0.8$, $\alpha_w = 2°$).

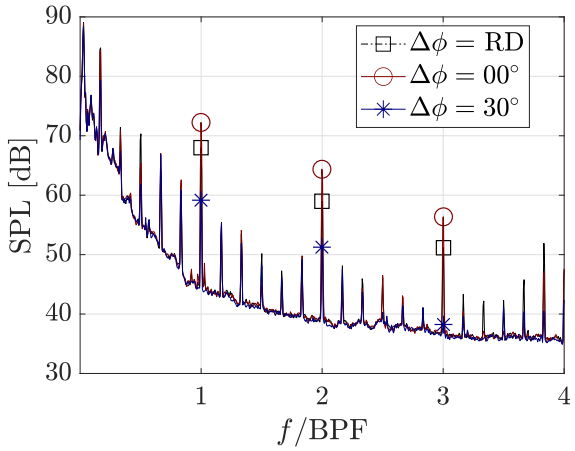

Fig. 7 Pressure spectra recorded on microphone C for $\Delta\phi$ = RD, 0° and 30°.

the random configuration, $\Delta\phi = 0°$ may result in a minor increase of 0.4 dB in noise in OSPL, and $\Delta\phi = 30°$ may result in a decrease of 1.5 dB at the microphone upstream. Nevertheless, downstream, the relative blade phase angle can have a more significant impact with a noise penalty of 3 dB at $\Delta\phi = 0°$ and a noise reduction of 4 dB at $\Delta\phi = 30°$ compared to the random configuration.

The changes in noise levels are primarily attributed to how the relative blade-phase angle ($\Delta\phi$) affects the aerodynamic interactions between the propellers. As $\Delta\phi$ changes from 0° to 30°, the aerodynamic interference between adjacent propellers decreases, reducing the strength of the noise sources and, subsequently, the noise emissions. Thus, compared to a random configuration, a $\Delta\phi$ of 30° would lower noise levels, while a $\Delta\phi$ of 0° would increase them. However, it is crucial to understand whether this trend persists when the angle of attack of the setup increases, which not only increases the incidence angle of the propeller, causing a higher asymmetric loading on the propeller disc, but also amplifies the aerodynamic impact of the wing on the propellers due to its upwash and blockage effect. The following subsection will discuss the implications of an increased angle of attack on the setup.

B. Angle of Attack Effect

Figure 9 shows the effect of increasing the angle of attack and adjusting the relative blade-phase angle on noise emissions. The advance ratio remains constant at 0.8 across all cases. The first row (Figs. 9a-9c) shows the OSPLs calculated at each of the 64 microphones at angles of attack 2°, 5°, and 8°, respectively. As expected, there is an increase

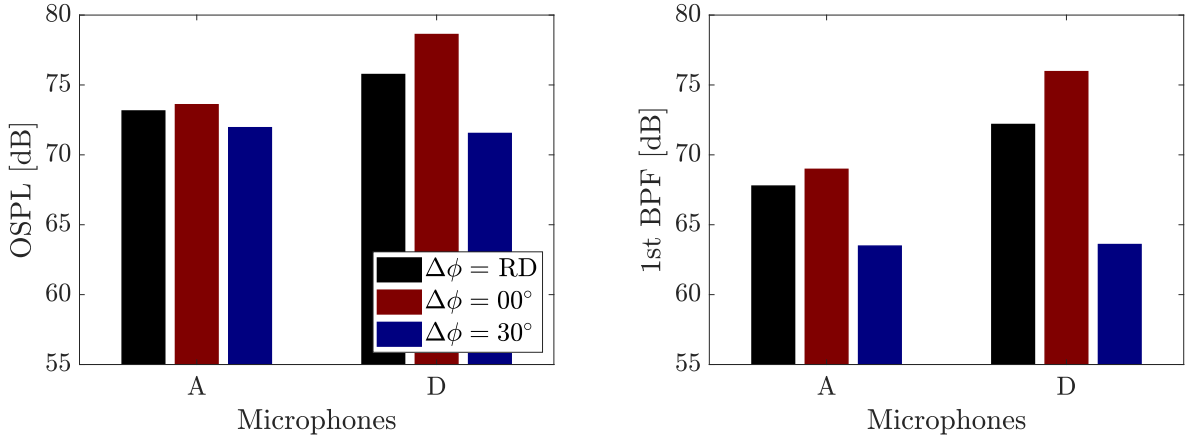

(a) Changes in OSPL. **(b) Changes at the first BPF.**

Fig. 8 Changes in sound levels in function of $\Delta\phi$ for microphones A and D.

in the noise levels in the microphones as the angle of attack increases. A higher angle of attack changes the airflow onto the propeller disc, creating an asymmetrical pattern. As the blades pass through this uneven inflow, they experience fluctuating aerodynamic forces, resulting in blade loading oscillation. The blades go through cycles of higher and lower loading with each rotation. This fluctuation affects the noise sources within the system, leading to a higher overall noise level. Therefore, an increased angle of attack intensifies these effects, resulting in higher noise emissions from the system. Thus, for the random case, OSPL_{avg} increases from 74 dB to 76 dB.

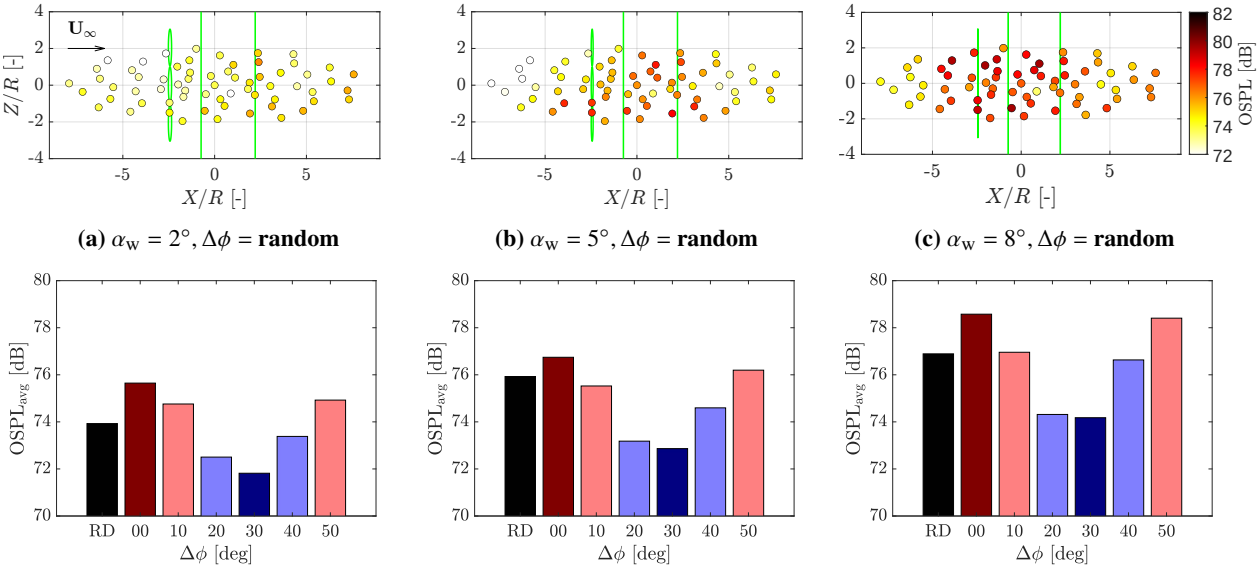

(a) $\alpha_w = 2°, \Delta\phi =$ **random** **(b)** $\alpha_w = 5°, \Delta\phi =$ **random** **(c)** $\alpha_w = 8°, \Delta\phi =$ **random**

(d) OSPL_{avg} ($\alpha_w = 2°$) **(e)** OSPL_{avg} ($\alpha_w = 5°$) **(f)** OSPL_{avg} ($\alpha_w = 8°$)

Fig. 9 Impact of relative blade phase angle $\Delta\phi$ in OSPL as the wing angle of attack increases.

The averaged OASPL at all microphones for each angle of attack, as illustrated in the second row of Fig. 9 (Figs. 9d-9f), shows how these values fluctuate with changes in the relative blade-phase angle. It is clear that different relative blade-phase angles can either increase or decrease the averaged OASPL compared to the random configuration. The highest values occur at 0°, while the lowest values are found at 30°. In the three cases, a relative blade-phase angle of 0° increases the average OASPL by approximately 1.5 dB compared to the values of the random case. Conversely, a relative blade-phase angle of 30° reduces the noise emissions by about 2 dB. Figure 9 shows that even with the impact

of a higher angle of attack, synchrophasing can effectively decrease the averaged OSPL of the system investigated.

IV. Conclusions

The research investigated the acoustic emissions of a distributed-propeller system in a tractor configuration, specifically exploring the effects of different relative blade phase angles and angles of attack. Preliminary results indicated that changes in the relative blade-phase angle impacted the noise emissions. Specifically, a blade-phase angle of 30° resulted in the quietest noise levels at the positions investigated, with a reduction of approximately 1.5 dB at the upstream microphone and a more substantial reduction of around 4 dB at the downstream microphone, compared to a random phase angle. This noise reduction is attributed to decreasing aerodynamic interference between adjacent propellers at this phase angle. The investigation further considered whether the impact of the relative blade-phase angle remained consistent at higher angles of attack. As the angle of attack increased, the noise levels decreased by about 2 dB at a 30° relative blade-phase angle compared to random-phase angles. In conclusion, the results imply that adjusting the relative blade-phase angle is a potential strategy for reducing noise emissions in a multi-propeller system. However, additional research is needed to determine if these results can be applied across an area beneath the configuration.

Funding Sources

This work is part of the ENODISE (ENabling Optimized Disruptive Airframe-Propulsion Integration Concepts) project, and has received funding from the European Union's Horizon 2020 research and innovation programme under grant agreement No. 860103.

References

[1] "Flightpath 2050 - Europe's Vision for Aviation," Tech. rep., 2011. https://doi.org/10.2777/50266.

[2] International Air Transport Association (IATA), "Aircraft Technology Net Zero Roadmap," Tech. rep., 2023. URL www.aviationbenefits.org.

[3] Stoll, A. M., Bevirt, J. B., Moore, M. D., Fredericks, W. J., and Borer, N. K., "Drag Reduction Through Distributed Electric Propulsion," *14th AIAA Aviation Technology, Integration, and Operations Conference*, Atlanta, GA, 2014, pp. 1–10. https://doi.org/10.2514/6.2014-2851.

[4] Kim, H. D., Perry, A. T., and Ansell, P. J., "A Review of Distributed Electric Propulsion Concepts for Air Vehicle Technology," *2018 AIAA/IEEE Electric Aircraft Technologies Symposium, EATS 2018*, 2018, pp. 1–21. https://doi.org/10.2514/6.2018-4998.

[5] Kim, H. D., Perry, A. T., and Ansell, P. J., "Progress in Distributed Electric Propulsion Vehicles and Technologies," 2020, pp. 1–44.

[6] Pascioni, K. A., Rizzi, S. A., and Schiller, N. H., "Noise Reduction Potential of Phase Control for Distributed Propulsion Vehicles," *AIAA Scitech 2019 Forum*, 2019, pp. 1–16. https://doi.org/10.2514/6.2019-1069.

[7] Barker, J. E., Zarri, A., Christophe, J., and Schram, C. F., "Numerical Investigation of Tonal Noise Emissions from Propeller-Wing Aerodynamic and Acoustic Interactions," *AIAA AVIATION 2023 Forum*, American Institute of Aeronautics and Astronautics, Reston, Virginia, 2023, pp. 1–12. https://doi.org/10.2514/6.2023-4056, URL https://arc.aiaa.org/doi/10.2514/6.2023-4056.

[8] Zarri, A., Koutsoukos, A., and Avallone, F., "Aerodynamic and Acoustic Interaction Effects of Adjacent Propellers in Forward Flight," *AIAA AVIATION 2023 Forum*, American Institute of Aeronautics and Astronautics, Reston, Virginia, 2023, pp. 1–16. https://doi.org/10.2514/6.2023-4489, URL https://arc.aiaa.org/doi/10.2514/6.2023-4489.

[9] Magliozzi, B., "Synchrophasing for Cabin Noise Reduction of Propeller-Driven Airplanes," *AlAA 8th Aeroacoustics Conference*, 1983, pp. 1–8. https://doi.org/10.2514/6.1983-717.

[10] Fuller, C. R., "Noise Control Characteristics of Synchrophasing. I - Analytical Investigation," *AIAA Journal*, Vol. 24, No. 7, 1986, pp. 1063–1069. https://doi.org/10.2514/6.1984-2369.

[11] Jones, J. D., and Fuller, C. R., "Noise Control Characteristics of Synchrophasing. II - Experimental Investigation," *AIAA Journal*, Vol. 24, No. 8, 1986, pp. 1271–1276. https://doi.org/10.2514/3.9431.

[12] Schiller, N. H., Pascioni, K. A., and Zawodny, N. S., "Tonal Noise Control Using Rotor Phase Synchronization," *The Vertical Flight Society - Forum 75: The Future of Vertical Flight - Proceedings of the 75th Annual Forum and Technology Display*, 2019.

[13] Patterson, A., Schiller, N. H., Ackerman, K. A., Gahlawat, A., Gregory, I. M., and Hovakimyan, N., "Controller Design for Propeller Phase Synchronization With Aeroacoustic Performance Metrics," *AIAA Scitech 2020 Forum*, 2020. https://doi.org/10.2514/6.2020-1494.

[14] Patterson, A. P., Ackerman, K. A., Hovakimyan, N., and Gregory, I. M., "Trajectory Generation for Distributed Electric Propulsion Vehicles with Propeller Synchronization," *AIAA Scitech 2021 Forum*, , No. January, 2021, pp. 1–10. https://doi.org/10.2514/6.2021-0586.

[15] Heidelberg, L. J., and Woodward, R. P., "Advanced Turboprop Wing Installation Effects Measured By Unsteady Blade Pressure and Noise." *NASA Technical Memorandum*, 1987. https://doi.org/10.2514/6.1987-2719.

[16] Sinnige, T., Ragni, D., Malgoezar, A. M., Eitelberg, G., and Veldhuis, L. L., "APIAN-INF: An Aerodynamic and Aeroacoustic Investigation of Pylon-Interaction Effects for Pusher Propellers," *CEAS Aeronautical Journal*, Vol. 9, No. 2, 2018, pp. 291–306. https://doi.org/10.1007/s13272-017-0247-2.

[17] Zawodny, N. S., Boyd, D. D., and Nark, D. M., "Aerodynamic and Acoustic Interactions Associated with Inboard Propeller-Wing Configurations," *AIAA Scitech 2021 Forum*, , No. January, 2021, pp. 1–23. https://doi.org/10.2514/6.2021-0714.

[18] Poggi, C., Bernardini, G., and Gennaretti, M., "Aeroacoustic Analysis of Wing-Mounted Propeller Arrays," *AIAA Aviation 2021 Forum*, 2021, pp. 1–13. https://doi.org/10.2514/6.2021-2236.

[19] Zhou, W., Ning, Z., Li, H., and Hu, H., "An Experimental Investigation on Rotor-To-Rotor Interactions of Small UAV," *35th AIAA Applied Aerodynamics Conference, 2017*, , No. June, 2017, pp. 1–16. https://doi.org/10.2514/6.2017-3744.

[20] de Vries, R., van Arnhem, N., Sinnige, T., Vos, R., and Veldhuis, L. L., "Aerodynamic Interaction Between Propellers of a Distributed-Propulsion System in Forward Flight," *Aerospace Science and Technology*, Vol. 118, 2021, pp. 1–20. https://doi.org/10.1016/j.ast.2021.107009.

[21] Zhong, S., Zhou, P., Chen, W., Jiang, H., Wu, H., and Zhang, X., "An Investigation of Rotor Aeroacoustics With Unsteady Motions and Uncertainty Factors," *Journal of Fluid Mechanics*, Vol. 956, 2023, p. A16. https://doi.org/10.1017/jfm.2022.1097, URL https://www.cambridge.org/core/product/identifier/S0022112022010977/type/journal_article.

[22] Pascioni, K. A., and Rizzi, S. A., "Tonal Noise Prediction of a Distributed Propulsion Unmanned Aerial Vehicle," *2018 AIAA/CEAS Aeroacoustics Conference*, 2018, pp. 1–18. https://doi.org/10.2514/6.2018-2951.

[23] Serpieri, J., "Cross-Flow Instability: Flow Diagnostics and Control of Swept Wing Boundary Layers," Ph.D. thesis, Delft University of Technology, 2018. https://doi.org/10.4233/uuid:3dac1e78-fcc3-437f-9579-048b74439f55, URL https://repository.tudelft.nl/islandora/object/uuid:3dac1e78-fcc3-437f-9579-048b74439f55?collection=research.

[24] Bento, H. F., Ragni, D., Avallone, F., Simons, D., and Snellen, M., "Acoustic Wall Treatments for Wind Tunnel Aeroacoustic Measurements," *Applied Acoustics*, Vol. 199, 2022, pp. 1–15. https://doi.org/10.1016/j.apacoust.2022.108989, URL https://doi.org/10.1016/j.apacoust.2022.108989.

[25] Bento, H., Vandercreek, C. P., Avallone, F., Ragni, D., Sijtsma, P., and Snellen, M., "Wall Treatments for Aeroacoustic Measurements in Closed Wind Tunnel Test Sections," , No. June, 2023, pp. 1–15. https://doi.org/10.2514/6.2023-4162.

[26] van Arnhem, N., de Vries, R., Sinnige, T., and Veldhuis, L., "TUD-XPROP-S propeller geometry," , Mar. 2022. https://doi.org/10.5281/zenodo.6355670, URL https://doi.org/10.5281/zenodo.6355670.

[27] van Arnhem, N., de Vries, R., Sinnige, T., Vos, R., Eitelberg, G., and Veldhuis, L. L., "Engineering Method to Estimate the Blade Loading of Propellers in Nonuniform Flow," *AIAA Journal*, Vol. 58, No. 12, 2020, pp. 5332–5346. https://doi.org/10.2514/1.J059485.

[28] Boermans, L. M. M., and Rutten, P. B., "Two-Dimensional Aerodynamic Characteristics of Airfoil NLF-MOD22 with Fowler Flap," Tech. rep., Delft University of Technology, 1995.

[29] Veldhuis, L. L. M., "Propeller Wing Aerodynamic Interference," Ph.D. thesis, Delft University of Technology, 2005.

[30] Sinnige, T., De Vries, R., Avallone, F., Ragni, D., Eitelberg, G., and Veldhuis, L. L., "Unsteady pylon loading caused by propeller-slipstream impingement for tip-mounted propellers," *Journal of Aircraft*, Vol. 55, No. 4, 2018, pp. 1605–1618. https://doi.org/10.2514/1.C034696.